Multi-machine Dimensionless Transport Experiments

D. C. McDonald[1], D. Elbeze[2], F. Imbeaux[2], H. Leggate[1], C. C. Petty[3], A. Sirinelli[2], J. A. Snipes[4], T. Takizuka[5], H. Urano[5] and JET-EFDA contributors[*]

[1]Euratom/UKAEA Fusion Association, Culham Science Centre, Abingdon, OX14 3DB, UK
[2]Euratom-CEA, CEA/DSM/DRFC, CEA Cadarache, Saint-Paul lez Durance, France
[3]General Atomics, PO Box 85608, San Diego, CA 92186, USA
[4]MIT Plasma Science and Fusion Center, Cambridge, MA 02139, USA
[5]Japan Atomic Energy Agency, Naka Fusion Institute, Naka 311-0193, Japan
[*]See the Appendix of M.L.Watkins *et al.*, Fusion Energy 2006 (Proc. 21st Int. Conf. Chengdu, 2006) IAEA, (2006)

e-mail contact of main author: dmcd@jet.uk

Abstract. Integrated dimensionless confinement studies have been performed recently on JET, C-Mod, JT-60U, DIII-D, and Tore Supra. Analysis of ELMy H-mode identity experiments on JET and C-Mod shows that, despite results indicating confinement falls as density approaches the Greenwald limit, Greenwald fraction is not a relevant parameter for confinement scaling, but that collisionality is. Studies on JT-60U show a fall in ELMy H-mode confinement with increasing β, contrasting with those on DIII-D and JET which showed a negligible effect. Analysis of a multi-machine database indicates that the differing results may be due to a change in β dependency with plasma shape. Tore Supra experiments show a negligible β effect on L-Mode confinement, suggesting that any β dependence observed in ELMy H-modes is related to the edge pedestal. Statistical studies of multi-machine core and edge confinement databases lead to an improved explanation of these results. The impact of these results on the understanding of plasma transport and its extrapolation to ITER will be discussed.

1. Introduction

If energy confinement is dominated by the physics of fully ionised plasmas then plasmas, with matched shape and *q*-profiles, have normalised energy confinement times which may be expressed as $\omega_{ci} \cdot \tau_E = F(\rho^*, \beta, \nu^*)$ [1]. Here, $\rho^* = \rho_{Ti}/a \propto T^{1/2}/aB$ is the normalised ion Larmor radius, $\beta = 2\mu_0 p/B^2 \propto nT/B^2$ the normalised plasma pressure, and $\nu^* = (\nu_{ie} R/a)/\omega_{Tbi} \propto na/T^2$ the normalised collision frequency. Different classes of transport models predict differing dependencies on these parameters [2]. In addition, plasmas with equal ρ^*, β, and ν^* have the same normalised confinement regardless of their size. For these reasons, dimensionless analysis provides a natural method for relating tokamak confinement experiments to plasma theory, and for extrapolating experimental results to next step machines. Combined JET, C-Mod, JT-60U, DIII-D and Tore Supra studies have been performed with this aim. Their results will be discussed in this paper.

2. The impact of normalised temperature on ELMy H-mode confinement

If atomic physics plays a role, then energy confinement becomes dependent upon an additional dimensionless parameter, which can be taken as T/ξ_a [3]. Here $\xi_a = m_e e^4/\hbar^2$ is the atomic unit of energy and so the parameter T/ξ_a describes plasma ionisation, which may play a role at the plasma edge. Previous multi-machine experiments [4] have indicated that confinement is dominated by fully ionised plasma physics, and so T/ξ_a is not required as an additional dimensionless parameter. However, more recently, the possibility of atomic physics impacting on energy confinement has resurfaced through its connection to the Greenwald density limit, $n_{gr} \propto I/a^2$ [5].

n_{gr} is the empirically derived density limit, which is believed to be strongly dependent on atomic physics at the edge. Consequently, to express the Greenwald density fraction, $F_{gr} = \overline{n_e}/n_{gr}$, in dimensionless parameters requires the inclusion of T/ξ_a, specifically, as $F_{gr} = (T/\xi_a)^{-1/2} \beta q/(\varepsilon\rho*)$. Experiments on several machines have shown that energy confinement, normalised to empirically derived confinement scalings, falls with increasing Greenwald density fraction, F_{gr}, over a large range of densities from $F_{gr} = 0.5 - 0.9$ [6]. This can be interpreted as energy confinement (i) being F_{gr} dependent or (ii) having a significantly different density dependence to the empirically derived confinement scalings. A F_{gr} dependence would suggest atomic physics plays a significant role in energy confinement [7,8]. If, instead, the density dependence is wrong, this will be reflected by an incorrect $\nu*$ scaling, the parameter which varies most strongly in a density scan.

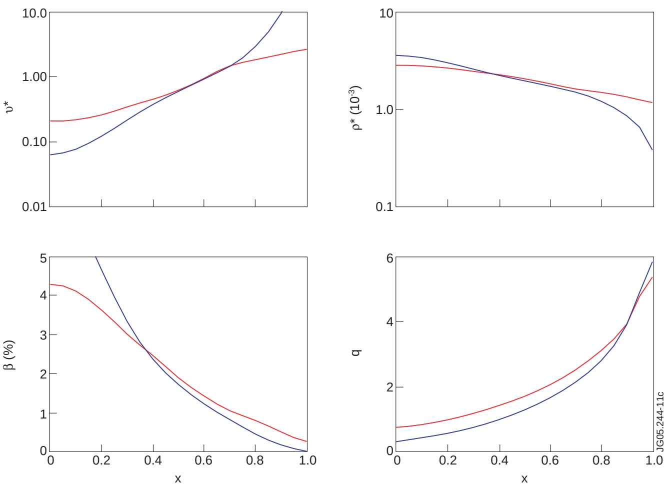

Figure 1. Profiles for JET shot #62663 (red/solid) and C-Mod shot #1001018013 (blue/dashed), showing matching of $\rho*$, β, $\nu*$ and q profiles. The x-coordinate is the normalised square root toroidal flux in all cases.

To test whether T/ξ_a or $\nu*$ is the dominant contributor to energy confinement, a plasma was produced on C-Mod and two plasmas, both with matched shape, were prepared on JET [9]. The first matched the C-Mod shot in $\rho*$, β, $\nu*$ and q, but had different T/ξ_a, or, equivalently, F_{gr}. To produce this match, the engineering variables scale with plasma minor radius as $B \propto a^{-5/4}$, $I \propto a^{-1/4}$, $n \propto a^{-2}$, $T \propto a^{-1/2}$ $\Rightarrow$ $T/\xi_a \propto a^{-1/2}$ and $F_{gr} \propto a^{1/4}$. If atomic physics were unimportant for confinement, this shot would be expected to have the same normalised confinement as the C-Mod shot. The second JET plasma matched the C-Mod shot in $\rho*$, β, T/ξ_a and q, but had different $\nu*$. To produce this match, the engineering variables scale with plasma minor radius as $B \propto a^{-1}$, $I \propto a^0$, $n \propto a^{-2}$, $T \propto a^0$ $\Rightarrow$ $\nu* \propto a^{-1}$. If atomic physics dominated the change in energy confinement with density, this shot would be expected to have matched confinement to the C-Mod one. A similar study had been performed between DIII-D and JET, but the scan had a smaller range in minor radius [8]. The wider range in machine size between C-Mod, $a = 0.22$ m, and JET, $a = 0.91$ m, ensured a clearer result.

Figure 1 shows the agreement between the resulting profiles for the two discharges with matched $\rho*$, β, $\nu*$ and q. The equivalent global measurements were all matched to within experimental errors, TABLE 1. The resulting range in T/ξ_a is over a factor of 2.1, with $F_{gr} = 0.55$ for C-Mod and $F_{gr} = 0.82$ for JET. The resulting normalised energy confinement time, $\omega_{ci} \cdot \tau_E \propto B \cdot \tau_E$, can be seen to agree to within 10%, less than the errors of the measurement. An analysis of local transport, indicates that normalised thermal diffusivity in the range $x = 0.4 - 0.8$ showed an equally good match. The profiles for the $\rho*$, β, T/ξ_a and q matches were found to agree to a similar degree. This time, however, the normalised energy confinement differs by a factor of over 2, TABLE 1. The local transport was consistent with the global transport, with the normalised thermal conductivity of the JET shot lying well below that of the C-Mod shot.

TABLE 1. COMPARISON BETWEEN THE GLOBAL PARAMETERS FOR THE JET AND C-MOD DISCHARGES WITH MATCHED $\rho*$, β AND (1) $\nu*$, (2) GREENWALD FRACTION

machine	**Shot no.**	**time [s]**	a	$\rho*/\rho*_{C-Mod}$	β/β_{C-Mod}	$\nu*/\nu*_{C-Mod}$	F_{gr}	$B \cdot \tau_E$ [Ts]
C-Mod	1001018013	1.26	0.22	1.00	1.00	1.00	0.55	0.28
JET (1)	62663	31.38	0.91	1.04	1.10	1.00	0.82	0.26
JET (2)	62657	34.68	0.91	0.96	0.98	0.28	0.58	0.69

The set of JET discharges was then extended by producing shots with similar $\rho*$, β and q profiles, but varying $\nu*$. The normalised energy confinement for all of the resulting shots is shown in **Error! Reference source not found.**a. It can be seen that the confinement in the JET shots has a strong, negative correlation with $\nu*$. A best fit curve gives $B \cdot \tau_E \propto \nu*^{-0.5\pm0.06}$. The matched C-Mod discharge fits into this scan. In contrast, when confinement for the same shots is plotted against F_{gr}, the correlation is less clear and the C-Mod shot falls outside the cloud, considerably below its matched JET discharge.

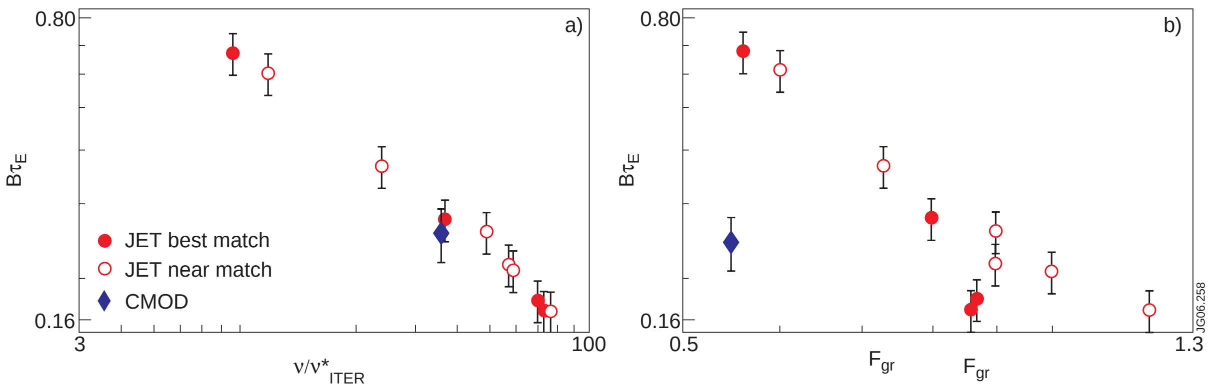

Figure 2: Normalised energy confinement time versus $\nu*$ (a) and Greenwald fraction (b) for a C-Mod discharge and JET discharges with matched $\rho*$, β, q profile and shape to the C-Mod discharge.

The results indicate that, for the parameter regime explored, confinement was found to be sensitive to changes in $\nu*$, but insensitive to changes in T/ξ_a, or, equivalently, F_{gr}. Thus, energy confinement appears to be dominated by the physics of fully ionised plasmas and atomic physics does not play a significant role. The observed fall in energy confinement, normalised to the empirically derived confinement scalings, with increasing Greenwald density fraction, F_{gr}, over the range from $F_{gr} = 0.5 - 0.9$, is instead ascribed to the confinement scalings missing some key physics. Dedicated $\nu*$ scans on JET [10], DIII-D [11], JT-60U [12], COMPASS-D [13] and C-Mod [14] found a range of power law scalings from $\omega_{ci}\tau_E \propto \nu*^{-0.3}$ at low $\nu*$ to $\omega_{ci}\tau_E \propto \nu*^{-0.8}$ at high $\nu*$. This indicates that the $\nu*$ dependence of energy confinement is not well represented by a power law, which may explain the apparent fall in normalised confinement with F_{gr}. As the $\nu*$ dependence originates from the competing turbulent transport processes, including TEM stabilisation and zonal flow damping, it seems likely that the $\nu*$ scaling would vary in different regions of parameter space.

3. The impact of β on ELMy H-mode confinement

For electrostatic turbulence models, the magnetic fields produced by the turbulence are assumed to be weak. As a result, their transport is largely independent of the parameter β, until β begins to approach the ideal ballooning stability limit [15]. Electromagnetic turbulent transport models, on the other hand, are strongly β dependent, with confinement usually decreasing with β. Thus, the β dependence of transport is a strong differentiator between electrostatic and electromagnetic turbulent transport models.

Experiments on ELMy H-modes in JET [16,17] and DIII-D [18,19] have shown no dependency of global energy confinement, or local transport, on β. These results appeared to show that the physics of global confinement was dominated by electrostatic turbulence models and was thus β independent in all cases. A recent study on JT-60U has contradicted this picture [20].

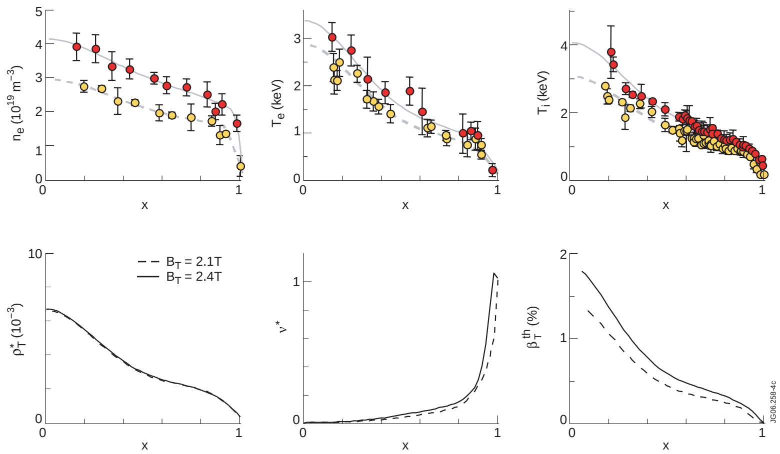

Figure 3 Radial profiles of (a) n_e,(b) T_e, (c) T_i , and the resulting (d) $\rho*$, (e) $\nu*$, and (f) β, for two of the discharges in the JT-60U β scans. In each case, the x-coordinate is the normalised toroidal flux.

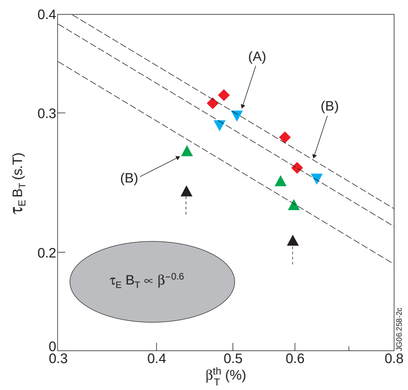

Figure 4. Normalised energy confinement time versus β for 3 sets of JT-60U shots with matched $\rho*$, $\nu*$, q profile and shape. A different symbol is used for each scan.

In the JT-60U experiments, as for the ones on JET and DIII-D, $\rho*$, $\nu*$ and q profiles were held fixed as β was varied by changing the magnetic field. To achieve this, the engineering parameters must be varied as $I \propto B$, $n \propto B^4$, and $T \propto B^2$. This was achieved for three sets of shots. Within each set, $\rho*$, $\nu*$ and q were thus fixed, but each set corresponded to a different $\rho*$, $\nu*$ and q. Hence, the sets constituted three independent β scans. The density and temperature profiles for two discharges in one of the scans, together with the derived $\rho*$, $\nu*$ and β profiles, are shown in Figure 3. $\rho*$ and $\nu*$ can be seen to be well matched.

The normalised confinement for all of these scans is plotted against β in Figure 4. It can be seen that for each scan, the normalised confinement falls with increasing β. A fit to these scans gives a scaling of $\omega_{ci}\tau_E \propto \beta^{-0.6}$. These JT-60U results clearly show a different β dependence of confinement to the virtually β independent results seen in the equivalent experiments on JET and DIII-D.

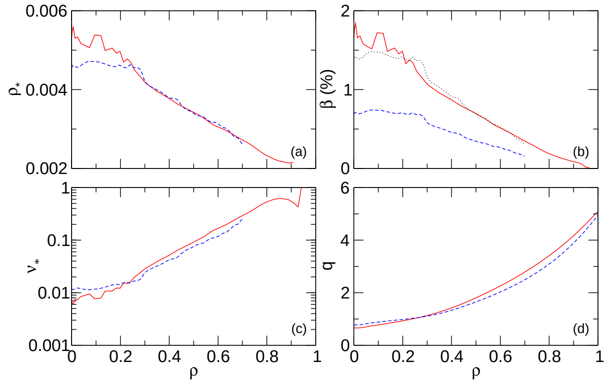

Figure 5. Radial profiles of $\rho*$, $\nu*$, β and q for two of the discharges in the Tore-Supra β scans. In each case, the x-coordinate is the square root normalised toroidal flux.

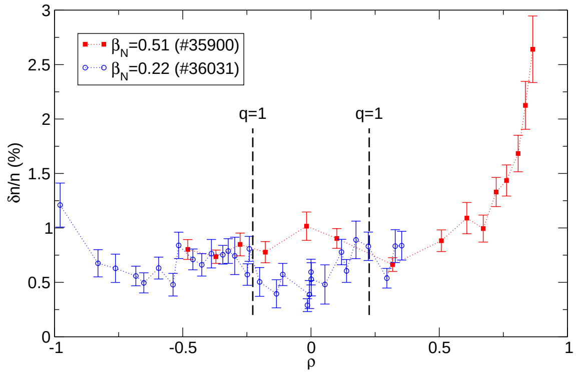

Figure 6. Radial profiles of the relative density fluctuations for a low (solid red squares) and high (open blue circles) β discharge from the Tore-Supra β scans. The x-coordinate is the square root normalised toroidal flux.

One possible impact of β on the ELMy H-mode confinement is through the edge pedestal region. This pressure gradient in this region is believed to be limited by the onset of ballooning modes and/or peeling modes, which are strongly dependent on β. To study the impact of β on confinement in the absence of an edge pedestal, an L-mode β scan was performed at Tore Supra [21]. Two discharges were produced at $B = 3.2$ T and a further two at $B = 3.8$ T, all with matched $\rho*$, $\nu*$ and q. This produced a β scan with a variation of a factor of 2. The match in the dimensionless parameter profiles is shown, for two of the discharges, in Figure 5. Outside of the core region, $\rho*$, $\nu*$ and q can be seen to be well matched. An analysis of the confinement of the discharges shows a weak β scaling, $\omega_{ci}\tau_E \propto \beta^{-0.2\pm0.2}$, close to previous TFTR [22] and DIII-D [18] results. Local transport analysis is consistent with this global scaling.

Density fluctuation measurements were also made for these discharges, using reflectometry. Profiles of the relative density fluctuations for a high and low β discharge from these β scans are shown in Figure 6. Outside of the $q < 1$ core region, where sawtooth activity pollutes the study of transport, the profiles are clearly well matched. Thus, the Tore-Supra experiment indicate that global confinement, local transport and turbulence are all, consistently, only weakly affected by β. This would suggest that any observed confinement degradation, such as in the JT-60U experiments, is likely to be due to an edge pedestal effect.

4. Consistency of dedicated experiments with the global multi-machine databases

The IPB98(y,2) scaling is derived from an Ordinary Least Squares (OLS) fit to the multi-machine H-mode database [23], and is expressed in engineering parameters as,

$$\tau_{IPB98(y,2)} = 5.62\times10^{-2} \cdot I^{0.93}B^{0.15}P^{-0.69}n^{0.41}M^{0.19}R^{1.97}\varepsilon^{0.58}\kappa_a{}^{0.78}. \quad (1)$$

Here, and in the other scalings, I is in MA, P is in MW, n is in $10^{19}\,\mathrm{m}^{-3}$, M is the ion mass relative to m_p, and the other variables are in SI units. This scaling is very close to satisfying the Kadomtsev constraint [1], and can be expressed in dimensionless parameters as,

$$\omega_{ci} \cdot \tau_{IPB98(y,2)} \propto \rho*^{-2.70}\ \beta^{-0.90}\nu*^{-0.01}\ M^{0.96}q^{-3.0}\varepsilon^{0.73}\kappa_a{}^{3.3}. \quad (2)$$

The strongly negative β dependence is clearly inconsistent with that observed in the JET and DIII-D results, and, indeed, is even stronger than seen in the JT-60U results. The negligible $\nu*$ dependency is inconsistent with all of the dedicated scans. Recent statistical reanalysis of the underlying database used for IPB98(y,2) has led to an improved fitting method, which gives a global scaling [24] of,

$$\tau_{EIV,Std} = 5.55\times10^{-2} \cdot I^{0.75}B^{0.32}P^{-0.62}n^{0.35}M^{0.06}R^{2.00}\varepsilon^{0.76}\kappa_a{}^{1.14}, \quad (3)$$

$$\omega_{ci} \cdot \tau_{EIV,Std} \propto \rho*^{-2.67}\ \beta^{-0.57}\nu*^{-0.14}\ M^{0.49}q^{-1.84}\varepsilon^{-0.19}\kappa_a{}^{3.34}. \quad (4)$$

Compared to the IPB98(y,2) scaling, this scaling has a weaker β dependence and more negative $\nu*$ dependence. The β dependence, intermediate to those observed in the dedicated multi-machine scans, results in a considerably better consistency between the new global scaling and the β scan experiments. However, by its simple power law nature, this scaling cannot reproduce the results from all the machines. A similar reanalysis of the L-mode database, has reduced its β scaling from $\omega_{ci}\tau_E \propto \beta^{-1.6}$ to $\omega_{ci}\tau_E \propto \beta^{-0.8}$ [25]. This brings the L-mode scaling into closer line with the dedicated β scans, but it still far from describing their β behaviour accurately. The similar density dependence of (3) to IPB98(y,2) means that it does not describe the density dependence of confinement seen in gas-fuelled discharges.

A more complete description of the observed β and $\nu*$ dependencies requires non-power law scalings. One class of such scalings are the "two-term" scalings, which separate the confinement properties of the core and pedestal region. A recent fit to a multi-machine database, restricted to ITER-like ($\kappa = 1.4-1.9$, $q_{cyl} = 1.6-2.8$) plasmas, gives a scaling of

$$\tau_{two-term,ITER-like} = 2.40\times10^{-2} \cdot I^{1.64}P^{-0.44}n^{-0.18}R^{1.03}\varepsilon^{-0.39} + 6.93\times10^{-2} \cdot I^{0.62}P^{-0.53}n^{0.64}R^{2.12}\varepsilon^{1.15}. \quad (5)$$

Such scalings do not naturally take dimensionless form, but, if $T_{core} >> T_{ped}$ and density profiles are approximately self-similar, (5) can be expressed in dimensionless parameters as,

$$\omega_{ci} \cdot \tau_{two-term,ITER-like} \propto \rho *^{-2.89} \beta^{-0.52} \nu *^{-0.59} + const \cdot \rho *^{-2.82} \beta^{0.25} \nu *^{-0.02} . \qquad (6)$$

In both expressions, the first term represents the pedestal and the second term the core confinement. For this scaling, both the β and $\nu *$ effects are stronger in the pedestal than in the core. However, neither the β or $\nu *$ dependencies of this scaling give a better description of those observed experimentally in Sections 2 and 3 than the standard power law scalings.

Analysis of the multi-machine database has also looked at the impact of plasma shape and gas fuelling on confinement [26]. This shows a correlation between the strength of the β degradation of confinement and plasma shape. The strongest degradation of confinement with β is associated with low upper triangularity, whereas β independence is associated with high upper triangularity. Gas fuelling is found to be correlated with poor confinement. For a set of JET plasmas, chosen to have $I_p \approx 2.5$ MA, the confinement, normalised to IPB98(y,2), for gas-fuelled discharges is found to be lower than for unfuelled discharges. This would seem to indicate a direct impact of fuelling on confinement, contradicting the results of the experiment discussed in Section 2. However, correlations between the amount of gas fuelling and the resultant collisionality, in the edge region, may explain this apparent contradiction. Comparative studies of pellet and gas fuelled discharges are required to resolve this.

5. Conclusion and future work

The results of Section 2 indicate that the inability of IPB98(y,2) to describe the dependence of confinement on density in gas-fuelled discharges does not imply that F_{gr} is a relevant parameter for confinement scaling. Instead, $\nu *$ is seen to be the critical parameter, but the $\nu *$ dependence in IPB98(y,2) is incorrect. Improved confinement scalings do not give a better representation of the density dependence. More experiments are planned to try to resolve the $\nu *$ scaling, including a JET ELMy H-mode $\nu *$ scan scheduled for 2006-7.

Studies on JT-60U show a fall in ELMy H-mode confinement with increasing β, contrasting with those on DIII-D and JET which showed a negligible effect. Analysis of a multi-machine database indicates that the differing results may be due to a change in β dependency with plasma shape. Tore Supra experiments have shown a negligible β effect on L-Mode confinement, suggesting that any β dependence observed in ELMy H-modes is related to the edge pedestal. A "two-term" core-pedestal confinement scaling supports this conclusion. Further non-power law dimensionless power law scalings should also be studied. Quadratic scalings, with terms like $\ln(\omega_{ci}\tau_E) \propto \ln(\nu *)^2 + A \cdot \ln(\beta) \cdot \ln(\delta)$ which naturally include the correlations discussed in this paper, are one possible form.

In addition to the future experiments outlined above, multi-machine $\rho *$ scans in ITER-like conditions, are planned for 2007. These will include C-Mod, JET, DIII-D and ASDEX-Upgrade in a one parameter extrapolation to ITER.

For ITER, the resolution of the $\nu *$ dependence of confinement would improve the confidence in present extrapolations to the lower collisionalities on ITER. Whilst not contradicting them, the identification of β dependent confinement adds a caution to extrapolating β independent scalings to predict high β, high performance regimes on ITER [19]. Further experimental and theoretical studies of dimensionless transport are expected to resolve these issues.

This work was partly supported by the United Kingdom Engineering and Physical Sciences Research Council and by the European Communities under the contract of Association between EURATOM and UKAEA. The views and opinions expressed herein do not necessarily reflect those of the European Commission. Part of this work is implemented under the International Energy Agency's cooperation agreement on Large Tokamak Facilities established between JAEA, US DOE, and EURATOM.

[1] B. B. Kadomtsev, Sov. J. Plasma Phys. **1** (1975) 295
[2] J. W. Connor and J. B. Taylor, Nucl. Fusion **17** (1977) 1047
[3] B. B. Kadomtsev, Comments Plasma Phys. Control. Fusion **13** (1989) 57
[4] T. C. Luce, *et al.*, Nucl. Fusion **42** (2002) 1193; and references therein
[5] M. Greenwald, *et al.*, Nucl. Fusion **28** (1988) 2199
[6] see for example, G. Saibene, *et al.*, Nucl. Fusion **39** (1999) 1133
[7] J. G. Cordey, *et al.*, Plasma Phys. Contr. Fusion **44** (2002) 1929
[8] C. C. Petty, *et al.*, Plasma Phys. Contr. Fusion **46** (2004) A207
[9] H. Leggate, *et al.*, "The significance of the dimensionless collisionality and the Greenwald fraction in the scaling of confinement", submitted to Nucl. Fusion
[10] J. G. Cordey, for the JET Team, "Energy confinement and H-mode power threshold scaling in JET with ITER dimensionless parameters", in Fusion Energy 1996 (Proc. 16th Int. Conf. Montréal, Canada, 1996) **1**, IAEA, Vienna (1997) 603
[11] C. C. Petty and T. C. Luce, Phys. Plasmas **6** (1999) 909
[12] H. Shirai, *et al.*, Plasma Phys. Contr. Fusion **42** (2000) 1193
[13] M. Valovic, *et al.*, "Energy Confinement of ELMy H-mode Plasmas on COMPASS-D Tokamak with ECR Heating", Proc. 26th EPS Conf. on Contr. Fusion and Plasma Phys., Maastricht, 1999, ECA **23J** (1999) 149
[14] M. Greenwald, *et al.*, Plasma Phys. Contr. Fusion **40** (1998) 789
[15] R. E. Waltz, *et al.*, Phys. Plasmas **4** (1997) 2482
[16] J. P. Christiansen and J. G. Cordey, Nucl. Fus. **38** (1998) 1757
[17] D. C. McDonald, *et al.*, Plasma Phys. Contr. Fusion **46** (2004) A215
[18] C. C. Petty, *et al.*, Nucl. Fus. **38** (1998) 1183
[19] C. C. Petty, *et al.*, Phys. Plasmas **11** (2004) 2514
[20] H. Urano, *et al.*, Nucl. Fusion **46** (2006) 781
[21] A. Sirinelli, *et al.*, "Turbulence measurements and local transport analysis in a dedicated Beta scan in Tore-Supra L-Mode discharges", Proc. 33rd EPS Conf. on Contr. Fusion and Plasma Phys., Rome, 2006
[22] S. D. Scott, "Nondimensional Transport Studies in TFTR", in Plasma Phys. Contr. Nucl. Fusion Res. (Proc. 14th Int. Conf., Germany, 1992) **3**, IAEA, Vienna (1993) 427
[23] ITER Physics Basis: Chapter 2, Nucl. Fusion **39** (1999) 2175
[24] D. C. McDonald, *et al.*, "Recent progress on the development and analysis of the ITPA global H-mode confinement database", submitted to Nucl. Fusion
[25] D. Elbèze, *et al.*, "Scaling of confinement in the ITPA L-mode database with dimensionless variables", Proc. 32nd EPS Conf. on Contr. Fusion and Plasma Phys., Tarragona, 2005, ECA **29C** (2005) P-1.033
[26] T. Takizuka, *et al.*, Plasma Phys. Contr. Fusion **48** (2006) 799